

## Article

# Influence of Dissolved Ions on the Water Purification Performance of TiO<sub>2</sub>-Impregnated Porous Silica Tubes

Mio Hayashi <sup>1</sup>, Tsuyoshi Ochiai <sup>1,2,3,\*</sup>, Shoko Tago <sup>1</sup>, Hiromasa Tawarayama <sup>4</sup>, Toshifumi Hosoya <sup>5</sup>, Tsukahara Yahagi <sup>6</sup> and Akira Fujishima <sup>1,3</sup>

<sup>1</sup> Photocatalyst Group, Research and Development Department, Local Independent Administrative Agency Kanagawa Institute of Industrial Science and Technology (KISTEC), 407 East Wing, Innovation Center Building, KSP, 3-2-1 Sakado, Takatsu-ku, Kawasaki, Kanagawa 213-0012, Japan;

pg-hayashi@newkast.or.jp (M.H.); pg-tago@newkast.or.jp (S.T.); fujishima\_akira@admin.tus.ac.jp (A.F.)

<sup>2</sup> Materials Analysis Group, Kawasaki Technical Support Department, KISTEC, Ground Floor East Wing, Innovation Center Building, KSP, 3-2-1 Sakado, Takatsu-ku, Kawasaki, Kanagawa 213-0012, Japan

<sup>3</sup> Photocatalysis International Research Center, Tokyo University of Science, 2641 Yamazaki, Noda, Chiba 278-8510, Japan

<sup>4</sup> Optical Communications R&D Laboratories, Sumitomo Electric Industries, Ltd., 1 Taya-cho, Sakae-ku, Yokohama 244-8588, Japan; tawarayama-hiromasa@sei.co.jp

<sup>5</sup> R&D General Planning Division, Sumitomo Electric Industries, Ltd., 1-1-3, Shimaya, Konohana-ku, Osaka 554-0024, Japan; t-hosoya@sei.co.jp

<sup>6</sup> Nanostructure Analysis Group, Kawasaki Technical Support Department, KISTEC, Ground Floor East Wing, Innovation Center Building, KSP, 3-2-1 Sakado, Takatsu-ku, Kawasaki, Kanagawa 213-0012, Japan; yahagi@newkast.or.jp

\* Correspondence: pg-ochiai@newkast.or.jp; Tel.: +81-44-819-2040; Fax: +81-44-819-2070

Academic Editors: Shaobin Wang and Xiaoguang Duan

Received: 27 April 2017; Accepted: 10 May 2017; Published: 16 May 2017

**Abstract:** TiO<sub>2</sub>-coated porous silica glass tubes containing macropores were fabricated and evaluated for their water-purification capacity using aqueous solutions of methylene blue. From the results of photocatalytic degradation tests at different initial methylene blue concentrations, the equilibrium adsorption constant ( $K$ ) was determined to be  $4.6 \times 10^{-2} \text{ L } \mu\text{mol}^{-1}$ , and the Langmuir-Hinshelwood rate constant ( $k_{LH}$ ) was calculated as  $2.6 \mu\text{M min}^{-1}$ . To determine the influence of ions on the efficiency of methylene blue degradation, we examined both Milli-Q water (soft water) and Contrex water (hard water) as solvents, and confirmed the reduced purification for the Contrex solution. It was, therefore, considered that the presence of inorganic salts decreased the photocatalytic efficiency. Furthermore, variations in the methylene blue decomposition ability were observed between anion-free and cation-free Contrex. Finally, we concluded that the efficiency of photocatalytic decomposition of TiO<sub>2</sub> was influenced by multiple parameters, including the presence of anions and cations, as well as the solution pH.

**Keywords:** photocatalyst; porous silica glass tube; water purification; hard water; TiO<sub>2</sub>

## 1. Introduction

Photocatalytic environmental purification has attracted a large amount of attention in recent years for the benefits of its low cost and enduring stability. On the other hand, commonly-used photocatalysts and photocatalytic filters are limited in their application because of relatively low purification efficiencies and difficulties in handling the powdered catalysts. Thus, although extensive research has been conducted on photocatalytic purification, the development of a practical purifier

is difficult and is still under investigation. To address this issue, we previously reported several methods for the design and application of a  $\text{TiO}_2$  photocatalyst to bring out its photocatalytic ability. [1,2]. In addition, we recently produced the simple and novel fabrication of one-end-sealed porous  $\text{TiO}_2$ -coated amorphous-silica (a-silica) tubes with high porosity using the outside vapor deposition (OVD) method [3]. In the case of  $\text{TiO}_2$  powders, such as P-25, it is difficult to separate the powder from the suspension and process it into a tube form, making it difficult to apply these materials to water purification. However,  $\text{TiO}_2$ -coated a-silica tubes have a self-supporting structure and are easy to handle. Evaluation of these tubes confirmed that they are suitable for the purification of both water and air. However, there are several important points regarding environmental conditions that must be contemplated when considering their application. For example, in the case of water purification, groundwater contains variable concentrations of inorganic ions, and so numerous studies have reported their effect on photocatalytic degradation [4–8].

We decided to evaluate the water purification ability of these tubes using Contrex, which is a hard water containing high quantities of ions. The porous a-silica tubes will initially be assayed for their water purification ability using the methylene blue decolorization test. We also aim to improve the water purification function of these tubes by evaluating the influence of dissolved ions. As such, the dissolved ions present in Contrex will be removed using an ion-exchange resin, and the resulting solutions will be used to evaluate the purification abilities of the tubes.

## 2. Results and Discussion

### 2.1. Characterization of Porous a-Silica Tubes

The manufacture of  $\text{TiO}_2$ -coated porous silica glass tubes was performed following our previously-reported method [9]. The average porosity and the average bulk density of the tubes were found to be 0.62 and 0.84 g/cm<sup>3</sup>, respectively. The specific surface area (BET) of porous silica glass tubes before coating  $\text{TiO}_2$  is approximately 7 m<sup>2</sup>/g. The pore diameter of the tubes in this research was estimated to be 0.4 µm. Back-scattered electron and Focused Ion Beam/Scanning Electron Microscopy (FIB/SEM) Serial Sectioning Nanotomography images (SEM: JSM-7800F Prime, JEOL Ltd., Tokyo, Japan) of a cross-section of a porous  $\text{TiO}_2$ -impregnated a-silica tube are shown in Figure 1. Modified  $\text{TiO}_2$  particles can be seen on the a-silica particles, with the white, grey, and black areas of Figure 1 representing  $\text{TiO}_2$  particles, a-silica particles, and the resin intruding in the pore, respectively.  $\text{TiO}_2$  existed on the surface of the a-silica skeleton even when it was located deep within a silica pore. It was also confirmed that  $\text{TiO}_2$  was not removed after decomposition tests. In addition, the 3D-models in Figure 1 show that the porous structure of the tube was relatively continuous in three dimensions. Raman spectroscopy indicated that the  $\text{TiO}_2$  particles in the  $\text{TiO}_2$ -impregnated a-silica tubes consisted of anatase crystals (Figure S1) [9].

### 2.2. Properties of the Methylene Blue Solutions

Table 1 shows the properties of the various solvents employed to prepare the methylene blue solutions used in the subsequent decomposition experiments. As Contrex is a type of hard water, it contains a large number of ionic species. As such, this solvent was passed through different ion-exchange resins to give “anion-free Contrex”, “cation-free Contrex”, and “ion-free Contrex,” the compositions of which are outlined in Table 1. In addition, after the removal of anions from the Contrex solution an increase in pH was observed due to an increase in the concentration of  $\text{OH}^-$  caused by the selectivity of this ion-exchange resin. Similarly, the cation-free Contrex solution exhibited a lower pH due to an increase in the concentration of protons.

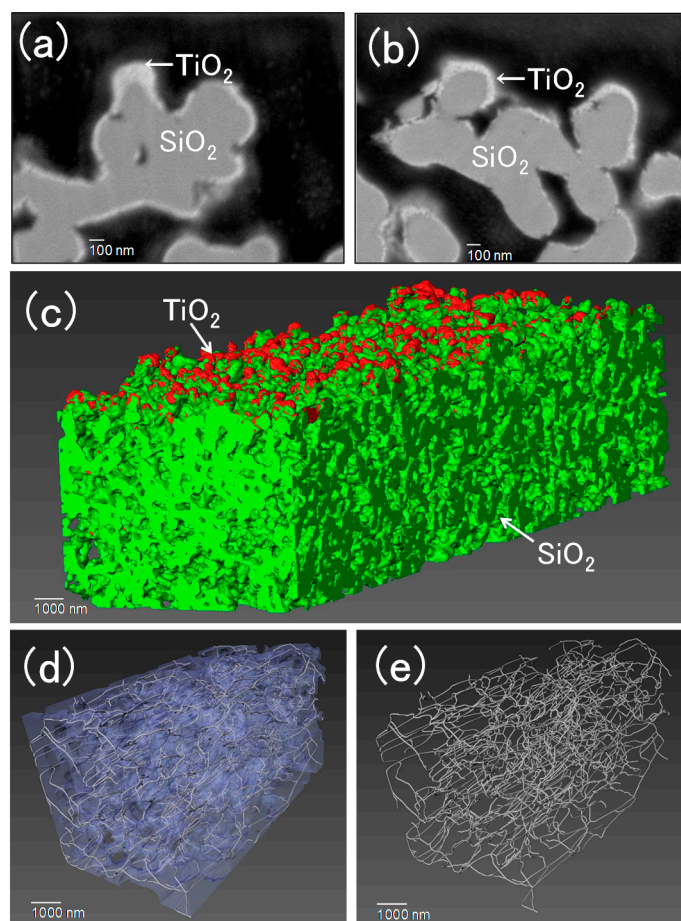


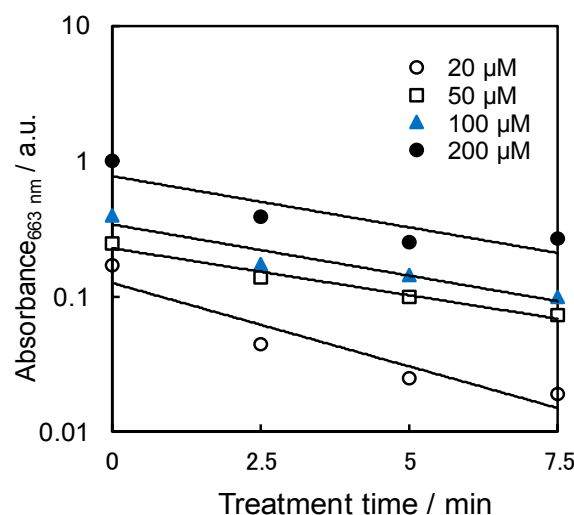
**Figure 1.** Back-scattered electron images of a cross-section of a porous  $\text{TiO}_2$ -impregnated a-silica tube (a) before decomposition tests and (b) afterwards. (c) Focused Ion Beam/Scanning Electron Microscopy (FIB/SEM) Serial Sectioning Nanotomography images calculated and reconstructed from SEM images of cross-sections of porous  $\text{TiO}_2$ -impregnated a-silica tubes. (d,e) are 3D-models of a small part of the structure shown in (c) that show (d) the porous structure of silica and (e) the pore structure.

**Table 1.** Properties of the solvents used to prepare the methylene blue solutions. The numbers in parentheses in the Contrex column represent the values quoted by the manufacturer. “n.d.” indicates “not detected”.

	Milli-Q	Contrex	Ion Exchanged Water	Anion-Free Contrex	Cation-Free Contrex	Ion-Free Contrex
Dissolved ion [mg/L]						
$\text{Ca}^{2+}$	0.0960	486 (468)	0.232	95.2	0.262	0.0143
$\text{Mg}^{2+}$	n.d.	82.2 (74.5)	0.005	n.d.	0.040	0.0255
$\text{Na}^+$	0.0328	8.0 (9.4)	0.037	3.00	0.774	0.021
$\text{K}^+$	n.d.	2.95 (2.8)	0.021	1.08	n.d.	0.010
$\text{SO}_4^{2-}$	n.d.	1356 (1121)	n.d.	1.30	1406	0.115
$\text{NO}_4^{2-}$	n.d.	2.76 (2.9)	n.d.	n.d.	2.51	n.d.
$\text{HCO}_3^-$	Unmeasured	Unmeasured (327)	Unmeasured	Unmeasured	Unmeasured	Unmeasured
$\text{Cl}^-$	n.d.	9.17 (7.6)	n.d.	3.29	11.0	n.d.
Electrical conductivity [ $\mu\text{S}/\text{cm}$ ]	0.91	1987	3.54	934	>1999	3.41
pH	7	7	7	11	2	7

### 2.3. Effect of Initial Methylene Blue Concentration

The effect of the initial methylene blue concentration was investigated by monitoring the absorbance at 663 nm, as shown in Figure 2. The different absorbance values obtained for the various concentrations at treatment times of 0 is due to the different methylene blue concentrations and the equilibrium developed prior to irradiation. From these data, the reaction rate constants ( $k_1$ ) of the TiO<sub>2</sub>-impregnated a-silica tubes were calculated to be 0.44, 0.44, 0.40, and 0.95 for the 200, 100, 50, and 20  $\mu\text{M}$  methylene blue solutions, respectively, indicating that, at high concentrations, the reaction rate constant remained relatively constant. The difference between the result at 20  $\mu\text{M}$  and those obtained at other concentrations can be explained by enhanced UV absorption by the dye molecules at high concentrations, which reduces the efficiency of the catalytic reaction due to the decrease in OH $\cdot$  and HO<sub>2</sub> $\cdot$  concentrations [10]. However, in this study, it appeared that the reaction rate constant did not exhibit a large decrease even at high methylene blue concentrations, likely due to the water passing through the tube forming a thin film, which subsequently underwent UV irradiation. This suggests that the design of our system acted to protect the photocatalyst.



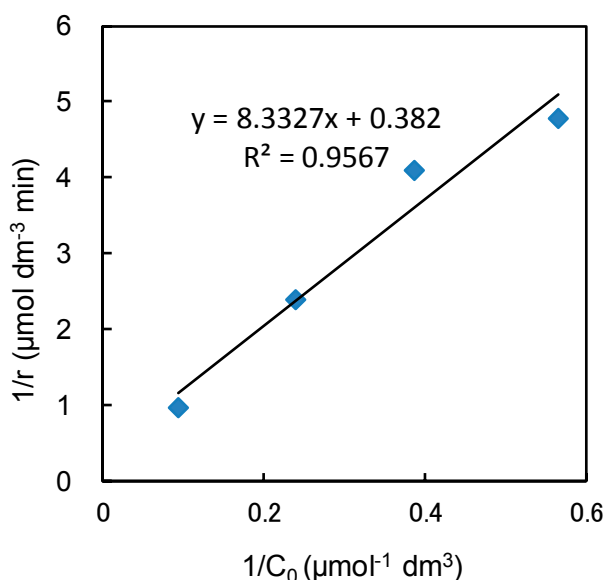
**Figure 2.** Effect of the initial methylene blue concentration present in Milli-Q water on photocatalytic removal at pH 7.

Figure 3 shows a plot of the inverse of the photodegradation rate ( $1/r$ ) versus the inverse of the saturated methylene blue concentration at each initial concentration ( $1/C_0$ ). As the photocatalytic oxidation kinetics of many organic compounds have been modelled using the Langmuir-Hinshelwood (L-H) equation [11,12], we assumed that the reaction took place at the surface of the photocatalyst particle, thus giving Equation (1):

$$r = k_{LH}KC_0/(1 + KC_0) \quad (1)$$

where  $k_{LH}$  is the Langmuir-Hinshelwood rate constant and  $K$  is the equilibrium adsorption constant. In addition, Ohtani reported that the isotherm is a function of the adsorbate concentration in solution, rather than the adsorbate concentration in the feed, as the Langmuir isotherm is derived based on the adsorption equilibrium between the adsorbed and desorbed species in solution [13]. Therefore, the equilibrium methylene blue concentration was applied to Equation (1) to give an estimated equilibrium adsorption constant ( $K$ ) of  $0.046 \mu\text{M}^{-1}$  and a Langmuir-Hinshelwood rate constant ( $k_{LH}$ ) of  $2.6 \mu\text{M min}^{-1}$ . These values are slightly different from the tendency reported for the conventional decomposition of methylene blue by a photocatalyst. For example, Sardar et al. reported a  $K$  value of  $0.08 \mu\text{M}^{-1}$  and a  $k_{LH}$  value of  $0.80 \mu\text{M min}^{-1}$  for the photodegradation of methylene blue using a TiO<sub>2</sub> suspension [14]. It is summarized that, in our experimental system,  $k_{LH}$  was high while  $K$  was relatively low. It was clear from the SEM images that the surface of the silica glass tubes used in our

experiment was not completely covered with  $\text{TiO}_2$ . This led to the lower  $K$  value seen in our system compared to that obtained in a system using a  $\text{TiO}_2$  suspension, as was used by Sardar et al. [14]. However,  $k_{LH}$  was three times larger in our system than when using a  $\text{TiO}_2$  suspension. This can be attributed to the predetermined quantity of methylene blue solution flowing through the porous silica tubes, which improved mass transfer efficiency and improved contact between the methylene blue and the  $\text{TiO}_2$  surface. Two of the authors of this article have previously reported a similar trend in the phenol decomposition process with a water-purification unit using  $\text{TiO}_2$ -impregnated quartz wool [15]. A reasonable  $k_{LH}$  value and a relatively smaller  $K$  value than that seen for the  $\text{TiO}_2$  suspension were obtained [11]. A similar mass transfer model and methylene blue supply to the  $\text{TiO}_2$  surface seemed to cause the reduced  $K$  value seen in the previous paper. Although the Langmuir-Hinshelwood model has previously only been applied to  $\text{TiO}_2$  suspensions, in this paper we applied the concept to a porous material. This resulted in a higher  $k_{LH}$  value than seen for the  $\text{TiO}_2$  suspension, with this being the first clear example of such behavior.



**Figure 3.** Plot of the inverse of the initial rate of photocatalytic degradation ( $1/r$ ) versus the inverse of the initial concentration of methylene blue ( $1/C_0$ ).

#### 2.4. Influence of the Dissolved Ions

As mentioned previously, natural mineral water contains variable concentrations of inorganic ions, which results in the formation of both soft and hard water. In this context, we employed both Milli-Q water (soft water) and Contrex water (hard water) for these studies, with Figure 4 illustrating the difference between these two types of water when used for the decomposition of 20  $\mu\text{M}$  methylene blue. In these plots, treatment times of 0 min show the absorbance when the methylene blue solution reached its adsorption equilibrium. As shown, the amount of adsorbed methylene blue is higher for Milli-Q water than Contrex water at the adsorption equilibrium, and the degradation efficiency of the Contrex system was significantly lower than that of the Milli-Q system at pH 7. It was, therefore, proposed that the dissolved ions present in Contrex affected the efficiency of the methylene blue decomposition process. Indeed, it has previously been reported that, at neutral and basic pH values, the decrease in  $\text{TiO}_2$  photoefficiency induced by the addition of inorganic salts was mainly due to the formation of an inorganic layer on the  $\text{TiO}_2$  surface, which inhibited methylene blue adsorption [4]. In addition, the inhibition effect of anions on the decomposition of organic compounds can be attributed to the competitive adsorption of reactants and anions on the catalyst [5]. We, therefore, believe that a similar mechanism took place in our system.

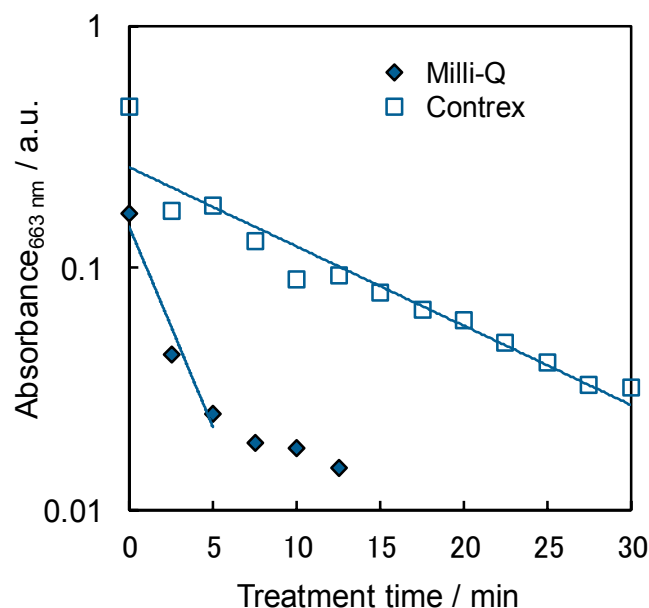


**Figure 4.** Photocatalytic degradation of methylene blue in Milli-Q and Contrex water.

As shown in Figure 5, the photocatalytic degradation of 20  $\mu\text{M}$  methylene blue in each solvent system was determined by measurement of the absorbance at 663 nm, which corresponds to the adsorption peak of methylene blue. These results confirmed the observations initially mentioned in this section, namely that the decomposition of methylene blue was enhanced in Milli-Q water compared to in Contrex water. As this was expected to be due to the presence of ions, the Contrex water was treated by passing it through various ion-exchange resins to remove anions, cations, or all ions from the solution, thus influencing the solution pH. As it has been previously reported that solution pH is a critical factor in determining the photocatalytic adsorption and degradation of organic compounds [7,16–18], we expected that the large difference between the pH values of the anion-free and cation-free Contrex solutions (see Table 1) would influence the photocatalytic ability of the  $\text{TiO}_2$  in our system.

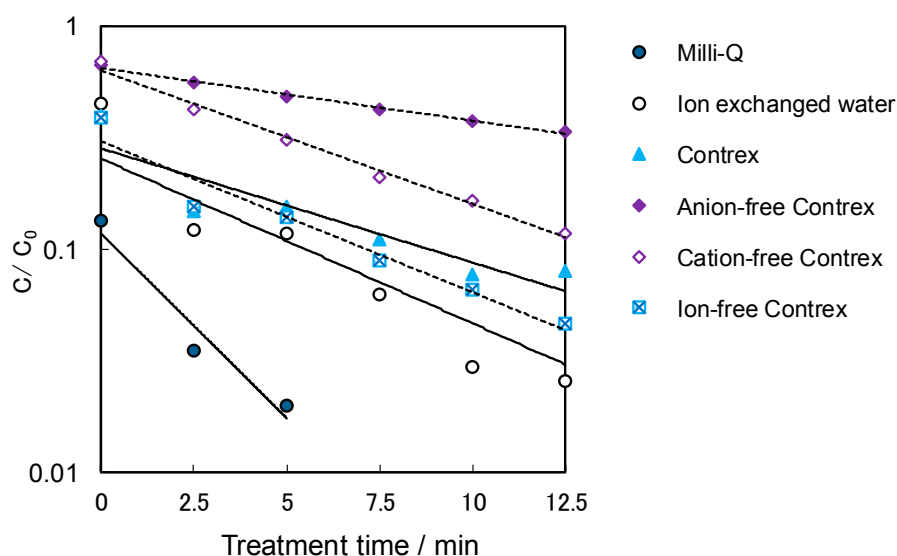


**Figure 5.** Photocatalytic degradation of methylene blue in the various aqueous solvents.



As mentioned above, solution pH can have a significant influence on the photocatalytic degradation of organic pollutants. More specifically, Shaban reported that the formation of  $\text{OH}^\bullet$  would be unfavorable under acidic conditions, thus leading to decreased photocatalytic degradation efficiency. It was also reported that, at high pH values ( $>8$ ), the formation of carbonate ions ( $\text{OH}^\bullet$  radical scavengers) was increased, which also reduced the efficiency of the photodegradation process. Thus, an optimum pH of 8 was recommended [17]. Furthermore, Guillard et al. reported that the increase in the photocatalytic efficiency of  $\text{TiO}_2$  at basic pH values was mainly attributable to an increase in the surface density of  $\text{TiO}^-$  adsorption sites, which attract methylene blue because of its cationic character [4]. However, our results indicated that the photocatalytic degradation of methylene blue in various types of water did not depend solely on the solution pH, but also on the presence of anions and cations in solution, thus suggesting a more complex system than that originally envisaged. In contrast, the photocatalytic degradation ability of the ion-free Contrex solution rose slightly in comparison with the non-treated Contrex solution. It is considered that the photocatalytic removal ability is a sum of methylene blue adsorption and photocatalytic decomposition efficiencies. A comparison of absorbance at the adsorption equilibrium and the reaction rate constant ( $k$ ) is shown in Figure 6. It was confirmed that decomposition and adsorption of methylene blue were higher in Milli-Q water than in the other solvents. In addition, removing both anions and cations from Contrex water increased the decomposition ability, providing results that were closer to those obtained using the ion-exchanged water. Furthermore, a large difference was seen between the absorption and decomposition results obtained using the Milli-Q water and the ion-exchanged water. This was considered to be due to the difference in electrical conductivity, with this being supported by the similarity between the ion-exchanged water results and those obtained using Contrex. These results, therefore, suggest that the dissolved ions present in water should be removed before photodegradation, thus leaving more sites available for the photocatalytic process.

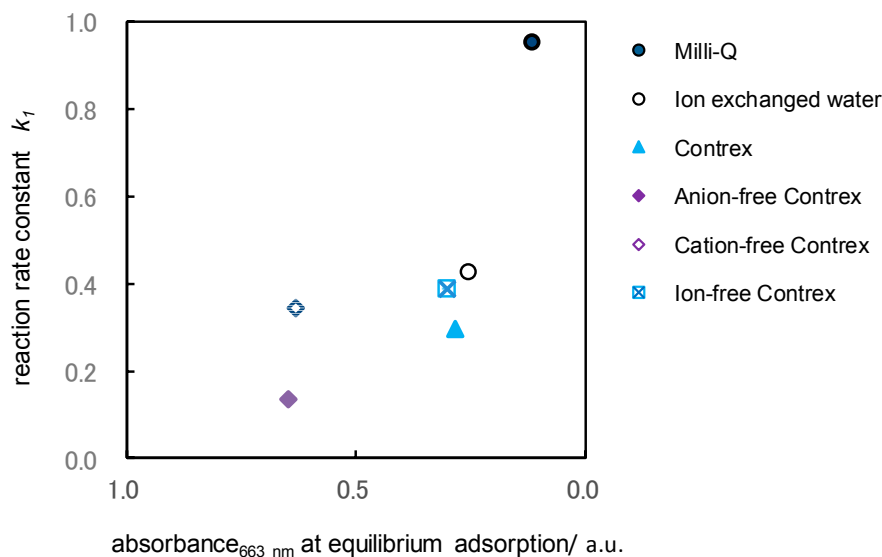
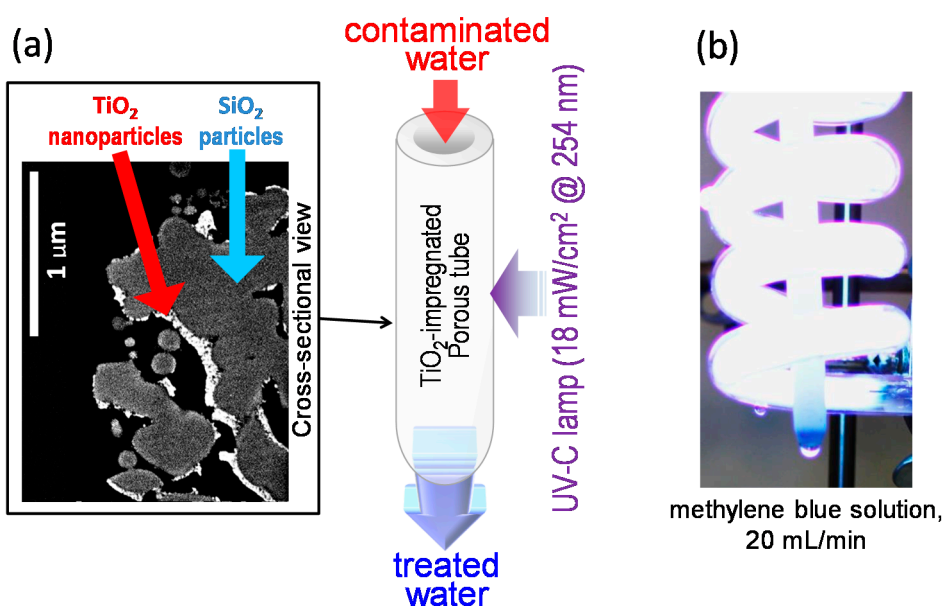


Figure 6. Comparison between the absorbances at adsorption equilibria and reaction rate constants ( $k$ ).

### 3. Materials and Methods

$\text{TiO}_2$ -impregnated porous silica tubes (external diameter = 8.6 mm, thickness = 1.3 mm) were prepared as previously described [9]. A schematic representation and a photograph of the methylene blue decomposition tests carried out using the  $\text{TiO}_2$ -impregnated porous a-silica tubes are shown in Figure 7. The methylene blue solutions were prepared using Milli-Q water (Merck Millipore Co., Darmstadt, Germany) as the soft water and Contrex as the hard water. In addition, the Contrex solvent was passed through anion-, cation-, and mixed-bed ion-exchange resins (Amberlite, ORGANO Co.,

Tokyo, Japan) to provide anion-free, cation-free, and ion-free solvents for use in the various experiments. The methylene blue solution (20–200  $\mu\text{M}$ ) was passed through the  $\text{TiO}_2$ -impregnated porous a-silica tube continuously to allow an adsorption equilibrium to be reached prior to treatment by UV irradiation. Subsequently, the decomposition of methylene blue on the  $\text{TiO}_2$ -impregnated porous a-silica tube was examined by passing a methylene blue solution (50 mL, 20–200  $\mu\text{M}$ ) through the tube at a flow rate of 20 mL/min under UV-C irradiation. The obtained solution was then stored in a beaker (Figure 7), and the ratio of methylene blue remaining was calculated by measuring the decrease in the absorbance at 663 nm using a Shimadzu UV-2450 UV-VIS spectrophotometer (Shimadzu Co., Kyoto, Japan). The stored/treated solution was then passed through the tube once again. Finally, the pseudo-first-order rate constants ( $k_1$ ) were calculated from the remaining ratios as a function of treatment times. The same  $\text{TiO}_2$ -coated porous silica glass tube was used throughout this report, and it was recycled by heat treatment (550  $^\circ\text{C}$ , 1 h) followed by ultrasonic cleaning after each decomposition test. In these experiments, a made-to-measure helical UV-C lamp (Kyokko Denki Co., Ltd., Tokyo, Japan) was employed as the UV light source, and a UV intensity value of 254 nm was maintained at the surface of the porous tube using a UVR-300 UV-radiometer equipped with a UD-250 sensor head (Topcon Corp., Tokyo, Japan). We have previously evaluated the antibacterial and antiviral properties of this silica glass tube using *Escherichia coli* and a Q $\beta$  phage, respectively [3], and by considering the combination of sterilization performance and photocatalyst performance, a wavelength of 254 nm was selected for these experiments.



**Figure 7.** (a) Schematic representation of the water purification test using the  $\text{TiO}_2$ -impregnated a-silica tube (right), and an SEM image of the cross-section of the tube (left). (b) Photograph of the water purification test. Reproduced from [9]. Copyright 2015, Catalysts.

#### 4. Conclusions

The photocatalytic ability of  $\text{TiO}_2$ -impregnated porous amorphous silica glass tubes containing micropores was investigated for the purification of water containing methylene blue. From the experimental results and discussion above, the following conclusions can be drawn:

##### (1) Application of the Langmuir-Hinshelwood (L-H) Model

The results of photocatalytic degradation tests using a range of methylene blue concentrations allowed us to use the Langmuir-Hinshelwood model to describe the photocatalytic performance of the tubes. More specifically, the equilibrium adsorption constant ( $K$ ) and the Langmuir-Hinshelwood



rate constant ( $k_{LH}$ ) were determined to be  $4.6 \times 10^{-2} \text{ L } \mu\text{mol}^{-1}$  and  $2.6 \mu\text{M min}^{-1}$ , respectively. These results, which show a low  $K$  value and a high decomposition efficiency, were likely a result of the improved mass transfer and contact efficiencies of methylene blue with the surface of the  $\text{TiO}_2$  silica tube.

## (2) Influence of dissolved ions

The photocatalytic ability of the system in both Milli-Q water and Contrex water was evaluated, and we found that the adsorption and photodegradation rate of methylene blue was significantly lower in Contrex water, which contained a number of inorganic ions. Following treatment of Contrex water with ion-exchange resins, the decomposition ability of the cation-free solvent (pH 2) was higher than that of the anion-free solvent (pH 11), although the decomposition ability of the non-treated Contrex water (pH 7) was superior to that of the ion-exchange-treated solvents. We, therefore, concluded that this complex process is affected not only by pH, but also by the presence of both anions and cations in solution. These results are expected to contribute to a better understanding of how environmental conditions can affect the photodegradation abilities of catalysts for the purification of groundwater.

**Supplementary Materials:** The following are available online at [www.mdpi.com/2073-4344/7/5/158/s1](http://www.mdpi.com/2073-4344/7/5/158/s1), Figure S1. Raman spectra of the  $\text{TiO}_2$ -impregnated a-silica tube.

**Author Contributions:** Mio Hayashi, Tsuyoshi Ochiai, Hiromasa Tawarayama, and Toshifumi Hosoya participated in the study design and conducted the study. Data was collected and analyzed by Mio Hayashi, Tsuyoshi Ochiai, Shoko Tago, Tsukaho Yahagi, and Hiromasa Tawarayama. The manuscript was written by Mio Hayashi. Akira Fujishima provided valuable discussions and advice regarding the manuscript.

**Conflicts of Interest:** The authors declare no conflict of interest.

## References

1. Liu, B.; Nakata, K.; Sakai, M.; Saito, H.; Ochiai, T.; Murakami, T.; Takagi, K.; Fujishima, A. Hierarchical  $\text{TiO}_2$  spherical nanostructures with tunable pore size, pore volume, and specific surface area: Facile preparation and high-photocatalytic performance. *Catal. Sci. Technol.* **2012**, *2*, 1933–1939. [CrossRef]
2. Reddy, K.R.; Nakata, K.; Ochiai, T.; Murakami, T.; Tryk, D.A.; Fujishima, A. Facile fabrication and photocatalytic application of Ag nanoparticles- $\text{TiO}_2$  nanofiber composites. *J. Nanosci. Nanotechnol.* **2011**, *11*, 3692–3695. [CrossRef] [PubMed]
3. Ochiai, T.; Tago, S.; Tawarayama, H.; Hosoya, T.; Ishiguro, H.; Fujishima, A. Fabrication of a porous  $\text{TiO}_2$ -coated silica glass tube and its application for a handy water purification unit. *Int. J. Photoenergy* **2014**, *2014*, 1–6. [CrossRef]
4. Guillard, C.; Puzenat, E.; Lachheb, H.; Houas, A.; Herrmann, J.-M. Why inorganic salts decrease the  $\text{TiO}_2$  photocatalytic efficiency. *Int. J. Photoenergy* **2005**, *7*, 1–9. [CrossRef]
5. Chen, H.Y.; Zahraa, O.; Bouchy, M. Inhibition of the adsorption and photocatalytic degradation of an organic contaminant in an aqueous suspension of  $\text{TiO}_2$  by inorganic ions. *J. Photochem. Photobiol. A* **1997**, *108*, 37–44. [CrossRef]
6. Jiang, Y.; Luo, Y.; Lu, Z.; Huo, P.; Xing, W.; He, M.; Li, J.; Yan, Y. Influence of inorganic ions and pH on the photodegradation of 1-methylimidazole-2-thiol with  $\text{TiO}_2$  photocatalyst based on magnetic multi-walled carbon nanotubes. *Bull. Korean Chem. Soc.* **2014**, *35*, 76–82. [CrossRef]
7. Wiszniowski, J.; Robert, D.; Surmacz-Gorska, J.; Miksch, K.; Weber, J.-V. Photocatalytic mineralization of humic acids with  $\text{TiO}_2$ : Effect of pH, sulfate and chloride anions. *Int. J. Photoenergy* **2003**, *5*, 69–74. [CrossRef]
8. Gjipalaj, J.; Alessandri, I. Easy recovery, mechanical stability, enhanced adsorption capacity and recyclability of alginate-based  $\text{TiO}_2$  macrobead photocatalysts for water treatment. *J. Environ. Chem. Eng.* **2017**, *5*, 1763–1770. [CrossRef]
9. Ochiai, T.; Tago, S.; Hayashi, M.; Tawarayama, H.; Hosoya, T.; Fujishima, A.  $\text{TiO}_2$ -impregnated porous silica tube and its application for compact air- and water-purification units. *Catalysts* **2015**, *5*, 1498–1506. [CrossRef]
10. Salehi, M.; Hashemipour, H.; Mirzaee, M. Experimental study of influencing factors and kinetics in catalytic removal of methylene blue with  $\text{TiO}_2$  nanopowder. *AJEE* **2012**, *2*, 1–7. [CrossRef]

11. Peiró, A.M.; Ayllon, J.A.; Peral, J.; Domenech, X. TiO<sub>2</sub>-photocatalyzed degradation of phenol and ortho-substituted phenolic compounds. *Appl. Catal. B* **2001**, *30*, 359–373. [[CrossRef](#)]
12. Ollis, D.F. Kinetics of liquid phase photocatalyzed reactions: An illuminating approach. *J. Phys. Chem. B* **2005**, *109*, 2439–2444. [[CrossRef](#)] [[PubMed](#)]
13. Ohtani, B. Chapter 10-Photocatalysis by inorganic solid materials: Revisiting its definition, concepts, and experimental procedures. In *Advanced Inorganic Chemistry: A Comprehensive Text*; van Eldik, R., Stochel, G., Eds.; Academic Press: Cambridge, MA, USA, 2011; Volume 63, pp. 395–430; ISBN: 0898-8838.
14. Sardar, S.; Sarkar, S.; Myint, M.T.; Al-Harhi, S.; Dutta, J.; Pal, S.K. Role of central metal ions in hematoporphyrin-functionalized titania in solar energy conversion dynamics. *Phys. Chem. Phys.* **2013**, *15*, 18562–18570. [[CrossRef](#)] [[PubMed](#)]
15. Ochiai, T.; Nakata, K.; Murakami, T.; Fujishima, A.; Yao, Y.Y.; Tryk, D.A.; Kubota, Y. Development of solar-driven electrochemical and photocatalytic water treatment system using a boron-doped diamond electrode and TiO<sub>2</sub> photocatalyst. *Water Res.* **2010**, *44*, 904–910. [[CrossRef](#)] [[PubMed](#)]
16. Zhang, J.; Cai, D.; Zhang, G.; Cai, C.; Zhang, C.; Qiu, G.; Zheng, K.; Wu, Z. Adsorption of methylene blue from aqueous solution onto multiporous palygorskite modified by ion beam bombardment: Effect of contact time, temperature, pH and ionic strength. *Appl. Clay Sci.* **2013**, *83–84*, 137–143. [[CrossRef](#)]
17. Shaban, Y.A. Enhanced photocatalytic removal of methylene blue from seawater under natural sunlight using carbon-modified n-TiO<sub>2</sub> nanoparticles. *Environ. Pollut.* **2013**, *3*, 41–50. [[CrossRef](#)]
18. Tolosa, N.C.; Lu, M.-C.; Mendoza, H.D.; Rollon, A.P. Factors affecting the photocatalytic oxidation of 2,4-dichlorophenol using modified titanium dioxide TiO<sub>2</sub>/KAl(SO<sub>4</sub>)<sub>2</sub> catalyst under visible light. *Sustain. Environ. Res.* **2011**, *21*, 381–387.



© 2017 by the authors. Licensee MDPI, Basel, Switzerland. This article is an open access article distributed under the terms and conditions of the Creative Commons Attribution (CC BY) license (<http://creativecommons.org/licenses/by/4.0/>).